XLVI CILAMCE
VITÓRIA - ES - BRAZIL - 2025
XLVI IBERO-LATIN AMERICAN CONGRESS ON COMPUTATIONAL METHODS IN ENGENEERING

# Experimental and Numerical Investigation of the Mechanical Behavior of Particulate Composite

Karen F. Timbó[1], Luiz A. T. Mororó[1,2], Marcelo S. M. Jr.[1], Evandro Parente Jr.[1]

[1]*Programa de Pós-Graduação em Engenharia Civil: Estruturas e Construção Civil, Universidade Federal do Ceará*
*Campus do Pici , 60455-900, Ceará, Brazil*
*karenft.eng@alu.ufc.br, marcelomedeiros@ufc.br, evandro@ufc.br*
[2]*Instituto Federal do Ceará*
*Campus de Fortaleza, Av. Treze de Maio, 60040-531, Fortaleza, Ceará, Brazil*
*luiz.mororo@ifce.edu.br*

**Abstract.** This study explores the mechanical characterization of a composite material consisting of polyester resin reinforced with silica particles. The analysis combines experimental tests and numerical modeling to investigate how different volume fractions (from 5% to 45%) influence the elastic properties of the composite. Laboratory tests provided the polymeric matrix parameters, while silica properties were determined through through data found in the literature. For numerical modeling, Representative Volume Elements (RVE) were developed in Abaqus along with the plugin EasyPBC, enabling the determination of elastic properties of the composite material. The obtained response was compared with established micromechanical models (Voigt, Reuss, Mori-Tanaka, Self-Consistent and Generalized Self-Consistent) to evaluate their applicability at different volume fractions. Results show that RVEs provide realistic estimates of the composite's global behavior, revealing the critical role of particle distribution and content in the material response. The methodology contributes to accurate prediction of mechanical properties and development of more efficient composite design strategies for specific applications.

**Keywords:** Characterization, Representative Volume Element, Micromechanical models.

## 1 Introduction

Composite materials have shown significant growth across various industrial sectors. Their mechanical, thermal, and functional versatility make them essential for aerospace, automotive, civil, mechanical, and electronic applications. It is well known that a material's microstructure strongly influences its macroscopic engineering response. Therefore, detailed understanding of the evolution, behavior, and mechanical response of materials at the microscopic level is fundamental.

The Representative Volume Element (RVE) approach is central to the homogenization of heterogeneous microstructures, such as composites, with the aim of predicting their effective properties. Furthermore, it is known that homogenization is the process of considering a statistically homogeneous representation of a heterogeneous material through a RVE. Many researchers have used and created definitions for this element. Hill [1] describes the RVE as a structurally typical sample containing a sufficient number of inclusions to ensure that the apparent moduli are independent of the boundary conditions. Hashin [2] complements this idea, stating that the RVE should be large enough to contain representative information about the microstructure, but much smaller than the macroscopic body. Thus, the RVE is a crucial factor for obtaining accurate predictions of a material's mechanical.

According to Pinho et al. [3], numerical analysis using an RVE is fundamental for the homogenization of composite materials with complex microstructures, allowing a heterogeneous medium to be modeled as an equivalent homogeneous medium. This process enables the determination of mechanical properties while reducing computational costs, which would be excessive in the direct modeling of complex geometries. This study investigate the elastic properties of a composite material composed of polyester resin with silica inclusions. The approach combines experimental and numerical methods, using microstructural modeling within the Finite Element Method (FEM) framework. To represent the heterogeneous structure of these materials, numerical models at the microscale are developed using RVEs. The study conducts numerous numerical analyses to perform statistical treatment and determine the most representative RVE, adopting a specific RVE for analyzing different inclusion

concentrations to obtain elastic properties of composite materials through homogenization using Abaqus [4]. Additionally, comparisons were made between numerical results and micromechanical models based on the Rule of Mixtures, Reuss, Mori-Tanaka, Self-Consistent and Generalized Self-Consistent, aiming to verify which models are most suitable depending on inclusion concentration, considering that some models are more accurate for lower particle concentrations.

## 2 Methodology

The methodology of this work combined experimental and numerical stages. In the experimental phase, laboratory tests were conducted to characterize the materials: pure polyester resin (matrix) was subjected to tensile and compression tests, while the silica inclusions underwent a granulometric analysis using the Shimadzu SALD-2300 equipment with the laser diffraction technique. This analysis determined a predominant particle diameter of 300 µm, an essential piece of data for developing dimensionally compatible RVE models. Finally, in the numerical stage, the elastic properties of the RVE models were compared with results from micromechanical homogenization models. The elastic properties of amorphous silica, such as Young's modulus (69–80 GPa) and Poisson's ratio (0.176–0.22), were extracted from the literature compiled by Vo et al. [5]. For the analyses, the values of 70 GPa and 0.2 were adopted, respectively, as they fall within this data range.

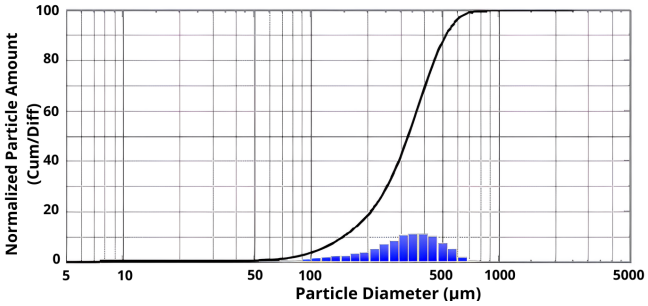



Figure 1. Cumulative particle size distribution curve (black) and differential (blue bars).

The mechanical properties of a composite can be determined using micromechanics-based models, which allows for the prediction of elastic, shear, and bulk moduli, as well as Poisson's ratio. Numerous homogenization models for composite materials are well-established in the literature, ranging from the simplest classical Voigt and Reuss models, the first of which is derived from the Rule of Mixtures (ROM), to intermediate models like Mori-Tanaka (MT), Self-Consistent (SC), Generalized Self-Consistent (GSC), and even more sophisticated computational models such as FEA and multiscale analysis ($FE^2$), depending on the desired analysis and the material under study. Thus, the numerical analysis of this work will address the Voigt and Reuss models based on the ROM, as well as the SC, GSC and MT models, which will serve as comparison parameters with the results obtained computationally through FEA using periodic boundary conditions with the help of the EasyPBC plugin [6] in Abaqus.

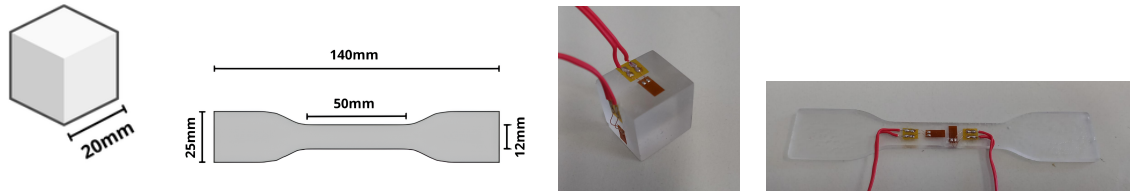
## 3 Experiments

The experimental analysis was the first stage of the methodology, based on laboratory tests to characterize the composite's constituent materials. Tensile and compression tests were performed on specimens to obtain material property data, in order to determine the elastic moduli and Poisson's ratio of the matrix composed of polyester resin. In contrast, the Young's modulus and Poisson's ratio of the silica particles were obtained from a review of literature data. The Poisson's ratio of the polyester resin was determined through the compression test, using a cubic specimen with a 2 cm edge and two strain gauges attached to measure the deformations. The tensile tests were performed on dog bones, whose extra dimensions are shown in Fig. 2, with thickness of 4 mm. The elastic properties of the polymeric matrix are: an elastic modulus ($E_m$) of 2.23 GPa and a Poisson's ratio ($\nu_m$) of 0.3. For the silica particles, the elastic modulus ($E_p$) is 70 GPa and the Poisson's ratio ($\nu_p$) is 0.2. The stress-strain curves obtained from the tensile and compression tests for the polyester resin are shown in Fig. 3.

## 4 Analytical Models

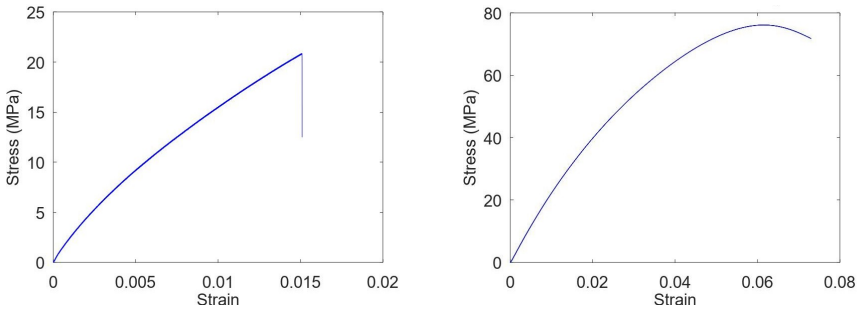
The mechanical properties of a composite can be determined using micromechanics-based models, allowing for the prediction of elastic, shear, and bulk moduli, as well as Poisson's ratio. In this work, the Voigt, Reuss,

MT, SC and GSC micromechanics and computational homogenization models, used to predict the mechanical properties of composites, will be used to compare the results obtained through a computational Finite Element Analysis (FEA) in Abaqus software [4].




(a) (b) (c) (d)

Figure 2. Specimens used in the experimental analysis: (a) and (b) show the specimen dimensions, while (c) and (d) show the compressive and tensile specimens.




(a) (b)

Figure 3. Tensile (a) and compressive (b) stress-strain curves.

### 4.1 Rule of Mixtures (ROM)

The ROM is the simplest method for predicting the mechanical properties of a material, described as the weighted average of the property to be determined, with the weights being the percentage concentrations of the material phases (typically two phases: matrix and particles/fibers). Thus, ROM is described by:

$$P = P_m V_m + P_p V_p, \tag{1}$$

where $P$ is the composite property, $P_m$ and $P_p$ refer to matrix and particle properties, while $V_m$ and $V_p$ are the volumetric fractions of matrix and particles.

From this ROM premise, we have the Voigt model [7], which considers uniform strain distribution within the material. In contrast, the Reuss model assumes uniform stress distribution, with property $P$ obtained as:

$$\frac{1}{P} = \frac{V_m}{P_m} + \frac{V_p}{P_p}. \tag{2}$$

### 4.2 Mori-Tanaka Model (MT)

The MT model [8] considers that the strain concentration tensor is exactly the same as for an RVE with a single inclusion, meaning inclusions in the RVE are subject to a far-field strain equal to the average matrix strain. For this model, the following formulations are used to determine the composite's mechanical properties. The composite's bulk modulus is obtained from:

$$K = K_m + \frac{V_p}{\frac{1}{K_p - K_m} + \frac{V_m}{K_m + \frac{4G_m}{3}}}, \tag{3}$$

where $K$ is the effective bulk modulus, and $K_m$ and $K_p$ represent the bulk modulus of the matrix and particle, respectively. $V_m$ and $V_p$ are the volume fractions of the matrix and and particle, respectively.

The shear modulus:

$$G = G_m + \frac{V_p}{\frac{1}{G_p - G_m} + \frac{V_m}{G_m + f_m}}, \tag{4}$$

where $G_m$ and $G_p$ are the shear modulus of the matrix and reinforcement, respectively, and $f_m$ is given by:

$$f_m = \frac{G_m(9K_m + 8G_m)}{6(K_m + 2G_m)}. \tag{5}$$

With the effective bulk (K) and shear (G) moduli determined, Young's modulus and Poisson's ratio can be obtained from:

$$E = \frac{9KG}{3K + G}, \tag{6}$$

$$\nu = \frac{3K - 2G}{2(3K + G)} \tag{7}$$

### 4.3 Self-Consistent Model (SC)

The SC model [9] uses an iterative method to determine the effective bulk ($K^*$) and shear ($G^*$) moduli. This process involves a series of repetitions that solve implicit equations, starting with an initial guess and refining the values at each iteration until the solution for the composite properties converges.

$$K^* = K_m + V_p\,(K_p - K_m)\,\frac{3K^* + 4G^*}{3K_p + 4G^*}, \tag{8}$$

$$G^* = G_m + V_p\,(G_p - G_m)\,\frac{15\,(1 - \nu^*)}{(7 - 5\nu^*) + 2\,(4 - 5\nu^*)\,(G_p/G^*)}, \tag{9}$$

where $K^*$, $G^*$ and $\nu^*$ are the effective bulk modulus, shear modulus, and Poisson's ratio, respectively.

### 4.4 Generalized Self-Consistent (GSC)

The Generalized Self-Consistent (GSC) method was developed by Christensen and Lo [10] for predicting the elastic properties of composite materials with spherical inclusions. The GSC geometric model is composed of three phases: a spherical inclusion, a spherical layer of matrix material, and an external homogeneous medium with the effective properties to be determined. To determine the composite's effective shear modulus, $\mu$, a quadratic equation must be solved that guarantees the continuity of stress and displacement conditions at the phase interfaces, given by:

$$\left(\frac{\mu}{\mu_m}\right)^2 A + \left(\frac{\mu}{\mu_m}\right) B + D = 0 \tag{10}$$

where $\mu_m$ represents the matrix's shear modulus. The polynomial coefficients, $A$, $B$, and $D$, are defined by complex expressions that depend on the properties of the phases and the volume fraction of the inclusions, as cited in the work of Christensen and Lo [10].

The coefficients and intermediate variables are calculated according to the equations present in the study by Christensen and Lo [10]. Once the effective shear modulus, $G$, is obtained from the quadratic equation's solution, the composite's Young's modulus ($E$) and Poisson's ratio ($\nu$) are determined through the standard relations of isotropic elasticity theory. It is worth noting that the effective bulk modulus ($K$) is calculated independently, and that from $K$ and $G$, the final properties of the composite are obtained by eq. (6) and eq. (7).

## 5 Numerical Models

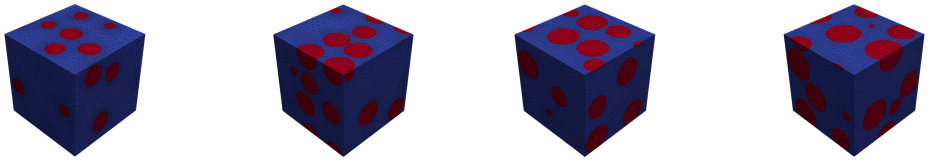
For the numerical analysis, a Python script was developed using the package GmshModel [11], a wrapper built on the native, Gmsh API [12] to simplify the creation of periodic RVE meshes. The generated mesh is composed of tetrahedral elements for a cubic RVE with spherical inclusions. The element size is controlled by refinement parameters that ensure an adequate adjustment near and between the inclusions, with an aspect ratio limited to 1.5. After generating the mesh, the Python code also produced an .inp file, which was imported into Abaqus, allowing the RVE to be analyzed using the EasyPBC plugin to determine the homogenized elastic properties of the composite material, providing values for the elastic modulus, shear modulus, and Poisson's ratio in the three material directions.

The EasyPBC plugin was developed by Omairey et al. [6], and is a tool for Abaqus that automates the calculation of the effective elastic properties of a periodic RVE. Its operation occurs in two stages: pre-processing, which organizes the RVE's geometry and applies the necessary constraints, and post-processing, which extracts data from the analysis to calculate the mechanical properties, such as stress, strain, and elastic moduli.The precision of EasyPBC [6] lies in how it applies periodic boundary conditions (PBCs), which are implemented node-to-node to allow the RVE's boundary surfaces to deform and distort, unlike other methods that forced them to remain planar and could overestimate the results. These conditions are applied through linear constraint equations that connect the nodal degrees of freedom. The material is considered isotropic in this analysis, and studies were conducted for different concentrations of silica in the polyester matrix (5% to 45% in 5% increments). The results were plotted to show the elastic modulus ($E$), the shear modulus ($G$), and Poisson's ratio ($\nu$) as a function of silica concentration (%), comparing them with analytical homogenization models.

To perform the computational finite element analyses using periodic boundary conditions, a study of the REV was conducted for each volume fraction of silica incorporated into the resin. Initially, five analyses were performed for the 20% RVE for each inclusion value considered, from 1 to 20 inclusions, totaling 100 models. The average elastic properties of the five models were then calculated for each number of inclusions, evaluating the percentage differences between the FEM model, the MT, SC and GSC models. It was possible to note that for the RVE with 13 or more inclusions, there was good convergence of the results. Thus, the REV with 15 silica inclusions was chosen to perform all the analyses in the Abaqus software using the EasyPBC plugin. In Figure 4, the meshes generated in the Python script with the package gmshModel [11] are shown. Table 1 shows the values corresponding to the edges ($a$) of the REV cube for each volumetric fraction of silica considered, represented in $mm$, and the volume ($V$) in $\mathrm{mm}^3$. It is important to note that the inclusions were considered to be spherical, with a diameter of 300 $\mu$m, according to the predominant particle size of the composite material's reinforcement, as determined by the granulometric analysis.

Table 1. Variation of RVE parameters with the percentage of inclusions.

| | 5% | 10% | 15% | 20% | 25% | 30% | 35% | 40% | 45% |
|---|---|---|---|---|---|---|---|---|---|
| a (mm) | 1.619 | 1.285 | 1.122 | 1.020 | 0.947 | 0.891 | 0.846 | 0.809 | 0.778 |
| V ($\mathrm{mm}^3$) | 4.241 | 2.121 | 1.414 | 1.060 | 0.848 | 0.707 | 0.606 | 0.530 | 0.471 |



(a) 10% (b) 20% (c) 30% (d) 40%

Figure 4. Finite element meshes obtained based on convergence studies, for the unit representative cells with reinforcement volume fractions of (a) 10%, (b) 20%, (c) 30%, (d) 40%.

## 6 Results and discussion

To compare the results obtained numerically through FEM, using periodic boundary conditions applied with the EasyPBC tool, with the other analytical models, three graphs were developed to provide a clear visualization of the mechanical properties: the longitudinal elastic modulus ($E$), the longitudinal shear modulus ($G$), and the principal Poisson's ratio ($\nu$).

As can be observed, the results obtained using finite elements (green) for the longitudinal elastic modulus in Fig. 5a shows a progressively increasing trend, starting at 2230 MPa for the material without any silica inclusions and reaching a maximum value of 5320.31 MPa for 45% silica content in the polyester matrix. It is also possible to note that the values obtained numerically with periodic boundary conditions (PBCs) are very close to the analytical results from the MT, SC, and GSC models up to 10%, with no discernible difference between the SC and GSC curves. Starting at 15%, the numerical model's data points are located between the lower bound represented by the GSC curve and the upper bound of the SC curve, up to approximately 35% silica content. From 40% onwards, the elastic properties show values between those obtained by the Reuss (red curve) and GSC (blue curve) models, with the 40% point being closer to the GSC model, and the 45% point being closer to the MT model.

Analyzing the graph in Fig. 5b, which shows the results for the shear modulus ($G$), it is possible to observe that the numerical values follow the same trend observed for the elastic modulus ($E$) up to approximately 35%. The FEM data points (green) are very close to those obtained using the MT model, and up to 10% there is practically no noticeable difference between the MT, SC, and GSC models. From 15% up to 35%, the numerical results are between the GSC and SC curves, and from 40% onwards, the values are between the MT and GSC curves. It is worth noting that the $G$ values increase, starting from 857.69 MPa for 0% silica and reaching 2170.28 MPa for 45% of reinforcement particles incorporated into the matrix.

Finally, Fig. 5c presents the results corresponding to the Poisson's ratio ($\nu$). Observing the FEM data points, it can be noted that they are located between the Reuss curve (red) and the SC curve (green) up to approximately 30%. From 35% onwards, the numerical model was positioned between the SC and MT curves, presenting practically the same value as SC for 35%, and a value very close to GSC for 45%. Regarding the numerical results, they do not follow a clearly increasing or decreasing pattern, but remain within a range of approximately 0.25 to 0.29, representing intermediate values between the Poisson's ratios of silica ($\nu = 0.2$) and the polyester matrix ($\nu = 0.3$).

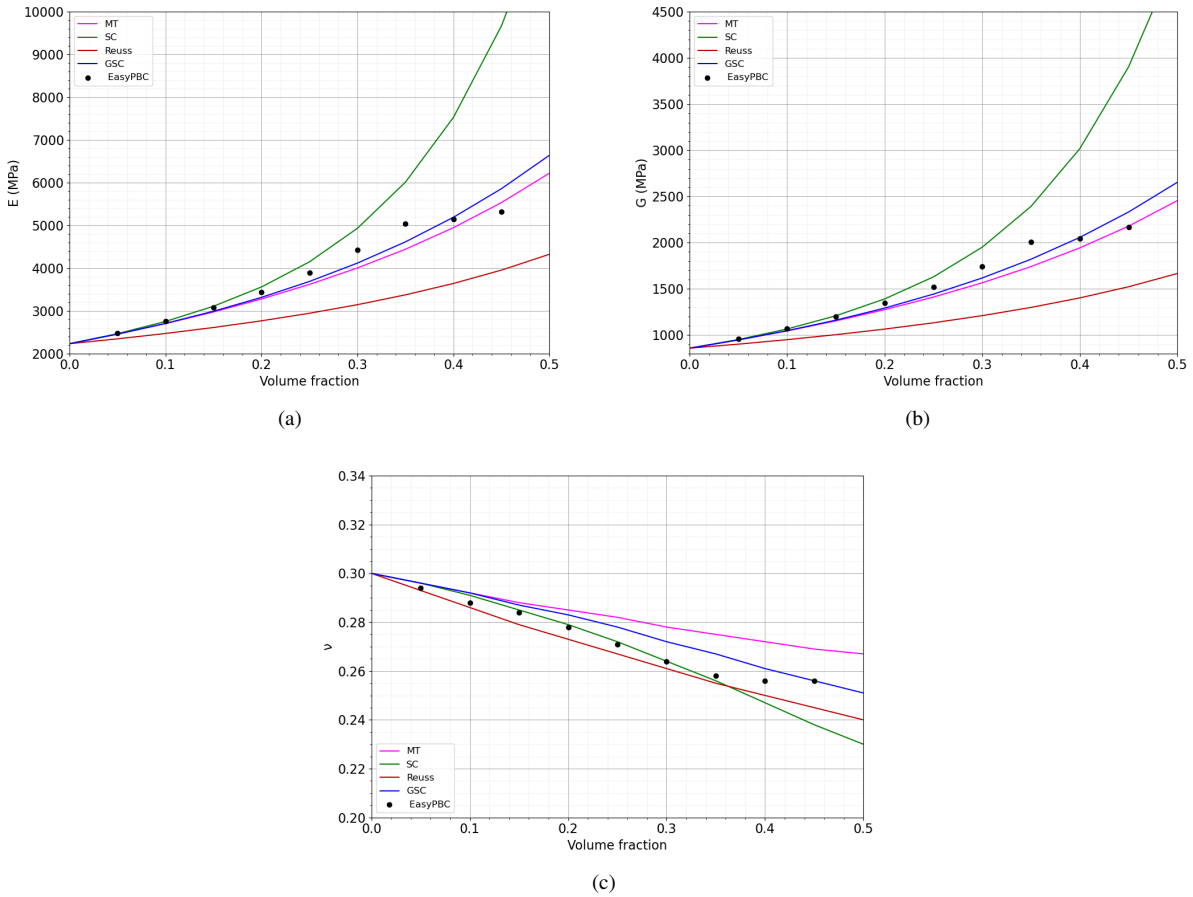



Figure 5. Comparison of the composite's homogenized properties as a function of silica concentration. (a) Longitudinal elastic modulus ($E$), (b) Longitudinal shear modulus ($G$), and (c) Major Poisson's ratio ($\nu$).

## 7 Conclusions

Based on the results of the graphs in Fig. 5a and Fig. 5b, the Generalized Self-Consistent (GSC) model has been shown to be, in general, the best analytical approximation for the numerical results of the FEM. The superiority of the GSC model can be attributed to its rigorous formulation, which, unlike other analytical models,

satisfies the continuity conditions at the phase interfaces. This model, developed by Christensen and Lo [10], was specifically designed to overcome the physical inconsistencies of simpler models and provide more accurate solutions for its three-phase model.

Nevertheless, the predictions of micromechanics models, including GSC, are limited for composites with high stiffness contrast and high volume fractions of reinforcement. It is also possible to observe that the accuracy of the SC micromechanics model relative to the numerical model significantly decreases in composites with high stiffness contrast and high volume fractions of reinforcement. This is corroborated by the knowledge that this model implicitly adopts the assumption of dilute dispersion, which disregards the effect of interaction between inclusions, and that the validity of this assumption disappears when the volume fraction is high. The literature aligns with this observation, demonstrating that the assumption of dilute dispersion is the fundamental source of the limitations, as stated by Luo [13]. Similarly, Christensen and Lo[14] states that the MT method lacks a rigorous theoretical basis and fails in highly concentrated conditions. This study, therefore, highlights the importance of more robust numerical approaches, such as the finite element method with periodic boundary conditions, to obtain accurate predictions of the elastic properties in scenarios where analytical models are not suitable.

**Acknowledgements.** The authors gratefully acknowledge the financial support provided by the Coordenação de Aperfeiçoamento de Pessoal de Nível Superior - Brasil (CAPES) - and Conselho Nacional de Desenvolvimento Científico e Tecnológico (CNPq).

**Authorship statement.** The authors hereby confirm that they are the sole liable persons responsible for the authorship of this work, and that all material that has been herein included as part of the present paper is either the property (and authorship) of the authors, or has the permission of the owners to be included here.

## References

[1] R. Hill. Elastic properties of reinforced solids: Some theoretical principles. *Journal of Mechanics and Physics of Solids*, vol. 11, n. 5, pp. 357–372, 1963.
[2] Z. Hashin. Analysis of composite materials: A survey. *Journal of Applied Mechanics*, vol. 50, n. 3, pp. 481–505, 1983.
[3] Pinho-da J. Cruz, P. Ferreira, J. Oliveira, and F. Teixeira-Dias. Homogeneização de propriedades de materiais compósitos em termoelasticidade linear. *Revista Iberoamericana de Ingeniería Mecánica*, vol. 13, n. 2, pp. 3–23, 2009.
[4] *Abaqus 2024 Documentation*. Dassault Systèmes Simulia Corp., Providence, RI, USA, 2024.
[5] T. Vo, B. Reeder, A. Damone, and P. Newell. Effect of domain size, boundary, and loading conditions on mechanical properties of amorphous silica: A reactive molecular dynamics study. *Nanomaterials*, vol. 10, n. 1, pp. 54, 2019.
[6] S. L. Omairey, P. D. Dunning, and S. Sriramula. Development of an abaqus plugin tool for periodic rve homogenisation. *Engineering with Computers*, vol. 35, pp. 567–577, 2019.
[7] W. Voigt. Ueber die beziehung zwischen den beiden elasticitätsconstanten isotroper körper. *Annalen der Physik*, vol. 274, n. 12, pp. 573–587, 1889.
[8] T. Mori and K. Tanaka. Average stress in matrix and average elastic energy of materials with misfitting inclusions. *Acta Metallurgica*, vol. 21, n. 5, pp. 571–574, 1973.
[9] R. Hill. A self-consistent mechanics of composite materials. *Journal of the Mechanics and Physics of Solids*, vol. 13, n. 4, pp. 213–222, 1965.
[10] R. M. Christensen and K. H. Lo. Solutions for effective shear properties in three phase sphere and cylinder models. *Journal of the Mechanics and Physics of Solids*, vol. 27, n. 4, pp. 315–330, 1979.
[11] P. Metsch, A. C. Hansen-Dörr, and O. T. Turan. gmshmodel. A mesh modelling interface to the Gmsh-Python-API, 2024.
[12] C. Geuzaine and J.-F. Remacle. *Gmsh Reference Manual*. Christophe Geuzaine and Jean-François Remacle, 2025.
[13] Y. Luo. An accuracy comparison of micromechanics models of particulate composites against microstructure-free finite element modeling. *Materials*, vol. 15, n. 11, pp. 1–18, 2022.
[14] R. M. Christensen and K. H. Lo. On the range of validity of the mori-tanaka method. *Journal of Applied Mechanics*, vol. 59, pp. 863–868, 1992.